EGU General Assembly 2020

Technische Universität München

Wrocław University of Environmental and Life Sciences

Precise Galileo orbit determination using combined GNSS and SLR observations

Grzegorz Bury[1], Krzysztof Sośnica[1], Radosław Zajdel[1], Dariusz Strugarek[1], Urs Hugentobler[2]

[1] Institute of Geodesy and Geoinformatics, Wrocław University of Environmental and Life Sciences, Grunwaldzka 53, 50-357 Wroclaw, Poland
[2] Institute for Astronomical and Physical Geodesy, Technical University of Munich, 80333, Munich, Germany

Quality of the Galileo orbits provided within the experimental products of the IGS multi-GNSS combined orbits

Galileo orbits combined in the frame of the IGS Multi-GNSS Experiment Pilot Project (MGEX) are characterized with the accuracy below 3 cm. Despite a good agreement with SLR, i.e., low standard deviation of SLR residuals, orbits still contain **systematic effects during eclipsing periods for all the Galileo (for |β| < 12.3°) and for the Galileo-IOV during |β| > 60°.**

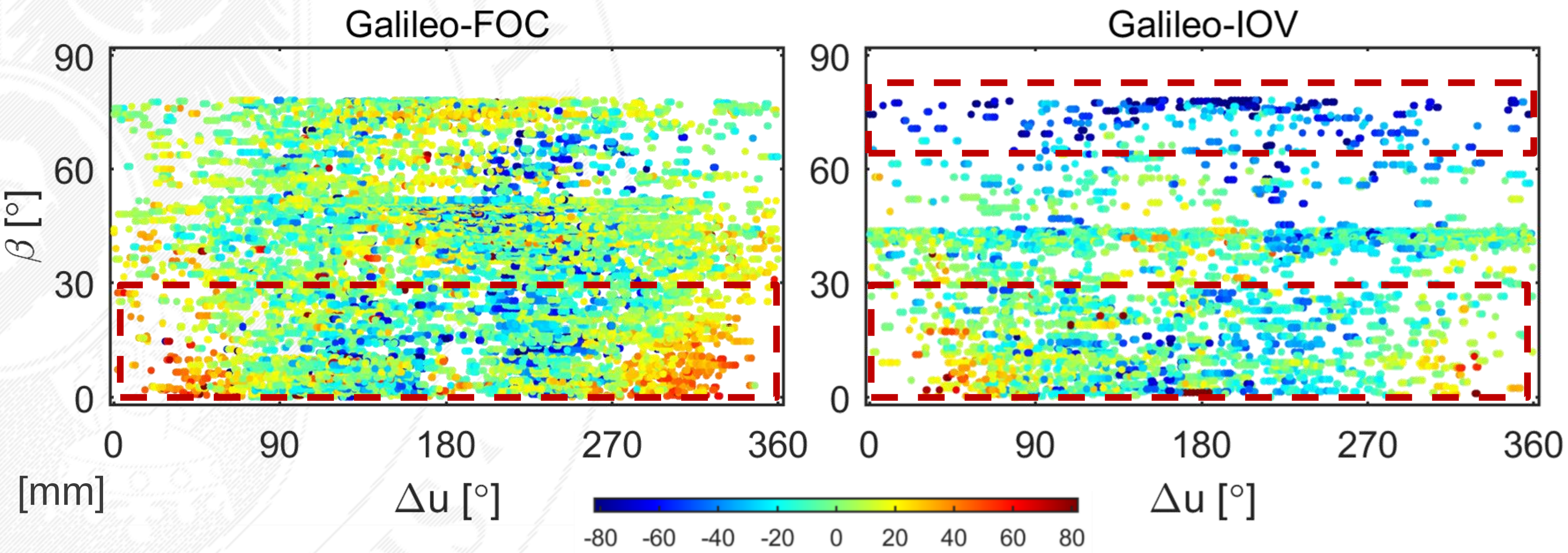

[mm]	IOV	FOC
Mean	-11	-1
STD	24	24

SLR residuals for the combined **Galileo orbits calculated in the frame of IGS MGEX** as a function of the Sun elevation above the orbital plane (β) and the argument of latitude of the satellite with respect to the argument of latitude of the Sun (Δu) for the period from April 29 to September 29, 2019

Sośnica K, Zajdel R, Bury G, et al (2020) Quality assessment of experimental IGS multi-GNSS combined orbits. GPS Solut 24:54. https://doi.org/10.1007/s10291-020-0965-5

Introduction of the box-wing model for the Galileo satellites

The box-wing model for the Galileo satellites significantly diminishes the STD of SLR residuals during the eclipsing periods (for |β| < 12.3°). However, a systematic offset is introduced.

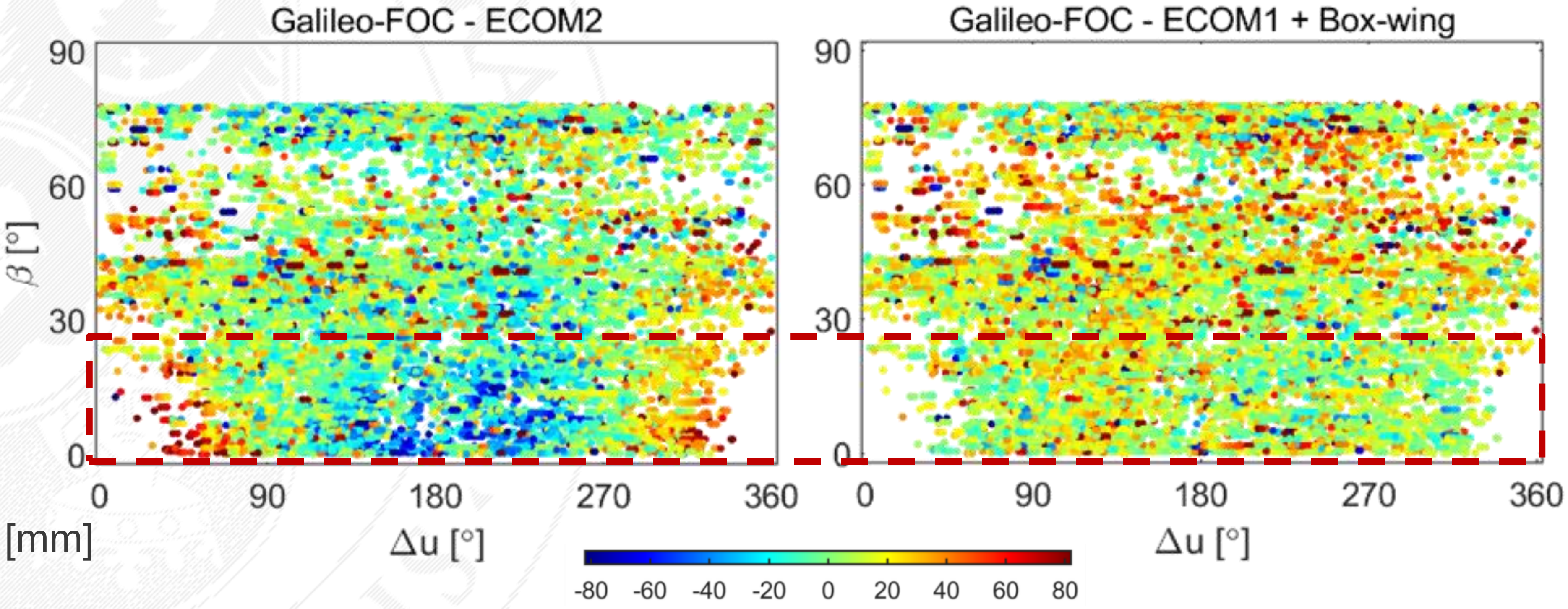

[mm]	FOC (ECOM2)	FOC (ECOM1 + Box-wing)
Mean	3.1	16.1
STD	27.3	25.0
STD |β|<12°	36.5	24.7

SLR residuals for the **Galileo-FOC orbits calculated using ECOM2 (left) and ECOM1 + Box-wing (right)** as a function of β and Δu for the period from January 1 to July 19, 2017

Bury G, Zajdel R, Sośnica K (2019) Accounting for perturbing forces acting on Galileo using a box-wing model. GPS Solut 23:74. https://doi.org/10.1007/s10291-019-0860-0

Motivation

- All **Galileo** satellites **are equipped** with the **Laser Retroreflector Arrays** for SLR.
- The International Laser Ranging Service **(ILRS) stations track the Galileo satellites**, e.g., in the frame of the special GNSS tracking campaigns.
- **SLR observations are typically used** as an independent technique **for the validation of the microwave orbit products**.
- Based **solely** on the **SLR observations**, it is possible to determine a **few-cm-level Galileo orbits**.

➢ **Can SLR data improve Galileo orbits?**

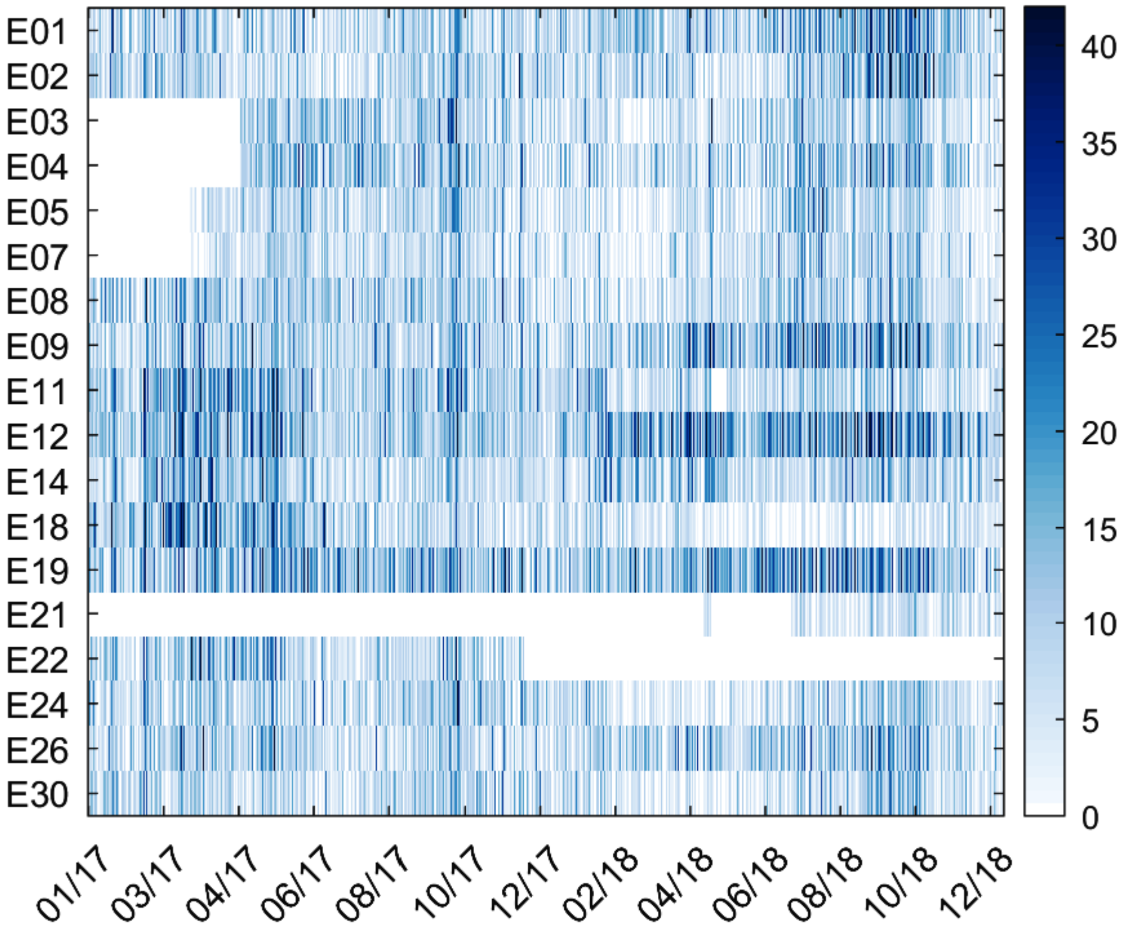

The number of the SLR observations to the particular Galileo satellite.

The goal of this study

- What is the **impact of the SLR observations** on the combined Galileo orbit solution?
- What is the **best weighting strategy** for the SLR observations?
- Can the addition of the SLR observations **help to mitigate the systematic errors** of the Galileo orbits?
- What is the **accuracy of the combined Galileo orbits**?

Processing strategy - models

Component	GNSS	SLR
Troposphere	Dry part: Vienna Mapping Function (Böhm et al. 2006), wet part: estimated	Dry and wet based on meteorological data (Mendes and Pavlis 2004)
Ionosphere	Modeled up to the third-order	-
Reference frame	IGS14	SLRF2014
Sat. antenna model	PCO and PCV from IGS/IGS MGEX (Steigenberger et al. 2016)	-
Rec. antenna model	Adopted from GPS L1 and L2 for Galileo	-
LRA offsets	-	Galileo metadata
Solid Earth tides	IERS2010 (Petit and Luzum 2010)	
Ocean tides	FES2004 (Lyard et al. 2006)	
Ocean tidal loading and geocenter corrections	FES2004, provided by Scherneck (1991)	
Solid Earth pole tides	IERS2010 based on Desai (2002)	
Mean Pole definition	IERS2010 (Petit and Luzum 2010)	
Solar radiation pressure	a priori box-wing model based on the Galileo metadata (Bury et al. 2020)	
Albedo + infrared radiation	CERES monthly maps (Wielicki et al. 1996)	
Antenna thrust	IOV: 155 W, FOC: 200 W	

Processing strategy - models

- Different sensitivity to the atmosphere for SLR and GNSS.

Component	GNSS	SLR
Troposphere	Dry part: Vienna Mapping Function (Böhm et al. 2006), wet part: estimated	Dry and wet based on meteorological data (Mendes and Pavlis 2004)
Ionosphere	Modeled up to the third-order	-
Reference frame	IGS14	SLRF2014
Sat. antenna model	PCO and PCV from IGS/IGS MGEX (Steigenberger et al. 2016)	-
Rec. antenna model	Adopted from GPS L1 and L2 for Galileo	-
LRA offsets	-	Galileo metadata
Solid Earth tides	IERS2010 (Petit and Luzum 2010)	
Ocean tides	FES2004 (Lyard et al. 2006)	
Ocean tidal loading and geocenter corrections	FES2004, provided by Scherneck (1991)	
Solid Earth pole tides	IERS2010 based on Desai (2002)	
Mean Pole definition	IERS2010 (Petit and Luzum 2010)	
Solar radiation pressure	a priori box-wing model based on the Galileo metadata (Bury et al. 2020)	
Albedo + infrared radiation	CERES monthly maps (Wielicki et al. 1996)	
Antenna thrust	IOV: 155 W, FOC: 200 W	

Processing strategy - models

- Different sensitivity to the atmosphere for SLR and GNSS.
- Dedicated settings for GNSS and SLR instruments.

Component	GNSS	SLR
Troposphere	Dry part: Vienna Mapping Function (Böhm et al. 2006), wet part: estimated	Dry and wet based on meteorological data (Mendes and Pavlis 2004)
Ionosphere	Modeled up to the third-order	-
Reference frame	IGS14	SLRF2014
Sat. antenna model	PCO and PCV from IGS/IGS MGEX (Steigenberger et al. 2016)	-
Rec. antenna model	Adopted from GPS L1 and L2 for Galileo	-
LRA offsets	-	Galileo metadata
Solid Earth tides	IERS2010 (Petit and Luzum 2010)	
Ocean tides	FES2004 (Lyard et al. 2006)	
Ocean tidal loading and geocenter corrections	FES2004, provided by Scherneck (1991)	
Solid Earth pole tides	IERS2010 based on Desai (2002)	
Mean Pole definition	IERS2010 (Petit and Luzum 2010)	
Solar radiation pressure	a priori box-wing model based on the Galileo metadata (Bury et al. 2020)	
Albedo + infrared radiation	CERES monthly maps (Wielicki et al. 1996)	
Antenna thrust	IOV: 155 W, FOC: 200 W	

Processing strategy - models

- Different sensitivity to the atmosphere for SLR and GNSS.
- Dedicated settings for GNSS and SLR instruments.
- The combination of two independent space techniques demands **consistent models** for orbit and data modeling.

Component	GNSS	SLR
Troposphere	Dry part: Vienna Mapping Function (Böhm et al. 2006), wet part: estimated	Dry and wet based on meteorological data (Mendes and Pavlis 2004)
Ionosphere	Modeled up to the third-order	-
Reference frame	IGS14	SLRF2014
Sat. antenna model	PCO and PCV from IGS/IGS MGEX (Steigenberger et al. 2016)	-
Rec. antenna model	Adopted from GPS L1 and L2 for Galileo	-
LRA offsets	-	Galileo metadata
Solid Earth tides	IERS2010 (Petit and Luzum 2010)	
Ocean tides	FES2004 (Lyard et al. 2006)	
Ocean tidal loading and geocenter corrections	FES2004, provided by Scherneck (1991)	
Solid Earth pole tides	IERS2010 based on Desai (2002)	
Mean Pole definition	IERS2010 (Petit and Luzum 2010)	
Solar radiation pressure	a priori box-wing model based on the Galileo metadata (Bury et al. 2020)	
Albedo + infrared radiation	CERES monthly maps (Wielicki et al. 1996)	
Antenna thrust	IOV: 155 W, FOC: 200 W	

Processing strategy - models

- Different sensitivity to the atmosphere for SLR and GNSS.
- Dedicated settings for GNSS and SLR instruments.
- The combination of two independent space techniques demands **consistent models** for orbit and data modeling.
- For all the solutions, we use the hybrid **ECOM1 and the box-wing model**, for the absorption of the direct Solar Radiation Pressure, albedo and IR.

Component	GNSS	SLR
Troposphere	Dry part: Vienna Mapping Function (Böhm et al. 2006), wet part: estimated	Dry and wet based on meteorological data (Mendes and Pavlis 2004)
Ionosphere	Modeled up to the third-order	-
Reference frame	IGS14	SLRF2014
Sat. antenna model	PCO and PCV from IGS/IGS MGEX (Steigenberger et al. 2016)	-
Rec. antenna model	Adopted from GPS L1 and L2 for Galileo	-
LRA offsets	-	Galileo metadata
Solid Earth tides	IERS2010 (Petit and Luzum 2010)	
Ocean tides	FES2004 (Lyard et al. 2006)	
Ocean tidal loading and geocenter corrections	FES2004, provided by Scherneck (1991)	
Solid Earth pole tides	IERS2010 based on Desai (2002)	
Mean Pole definition	IERS2010 (Petit and Luzum 2010)	
Solar radiation pressure	a priori box-wing model based on the Galileo metadata (Bury et al. 2020)	
Albedo + infrared radiation	CERES monthly maps (Wielicki et al. 1996)	
Antenna thrust	IOV: 155 W, FOC: 200 W	

Processing strategy – estimated parameters

Parameter	GNSS	SLR
Station coordinates	X, Y, Z for each GNSS and SLR station with NNR/NNT constraints for datum defining stations	
Datum defining stations for NNR/NNT	GNSS stations for which residuals of the Helmert transformation do not exceed 1 cm for the horizontal and 3 cm for the vertical coordinates	Set of the SLRF2014 core stations reduced by stations showing systematic effects McDonald (7080), Changchun (7237), Wettzell (8834) excluded
Pole coordinates	X pole, Y pole; two parameters per each component per day	
UT1-UTC	Initial value fixed to the a priori from IERS-14-C04, drift of the UT1-UTC freely estimated (denoted as LoD)	
Geocenter coordinates	X, Y, Z per each day	
Orbital elements	GNSS orbit parameters: 6 Keplerian, 5 ECOM: D_0, Y_0, B_0, B_{1C}, B_{1S} + stochastic orbit parameters in the radial, along-track, and cross-track directions every 12 h	
Troposphere	Site-specific zenith total delay (1 h), gradients (12 h)	-
Range Biases	-	Annual range biases calculated for each satellite-station pair; resubstituted and strongly constrained to a priori in the combined solution

Software: Bernese GNSS Software, modified version

Processing strategy – estimated parameters

- **Common parameters** – one set estimated based on two types of observations.

Parameter	GNSS	SLR
Station coordinates	X, Y, Z for each GNSS and SLR station with NNR/NNT constraints for datum defining stations	
Datum defining stations for NNR/NNT	GNSS stations for which residuals of the Helmert transformation do not exceed 1 cm for the horizontal and 3 cm for the vertical coordinates	Set of the SLRF2014 core stations reduced by stations showing systematic effects McDonald (7080), Changchun (7237), Wettzell (8834) excluded
Pole coordinates	X pole, Y pole; two parameters per each component per day	
UT1-UTC	Initial value fixed to the a priori from IERS-14-C04, drift of the UT1-UTC freely estimated (denoted as LoD)	
Geocenter coordinates	X, Y, Z per each day	
Orbital elements	GNSS orbit parameters: 6 Keplerian, 5 ECOM: D_0, Y_0, B_0, B_{1C}, B_{1S} + stochastic orbit parameters in the radial, along-track, and cross-track directions every 12 h	
Troposphere	Site-specific zenith total delay (1 h), gradients (12 h)	-
Range Biases	-	Annual range biases calculated for each satellite-station pair; resubstituted and strongly constrained to a priori in the combined solution

Software: Bernese GNSS Software, modified version

Processing strategy – estimated parameters

- **Common parameters** – one set estimated based on two types of observations.

Parameter	GNSS	SLR
Station coordinates	X, Y, Z for each GNSS and SLR station with NNR/NNT constraints for datum defining stations	
Datum defining stations for NNR/NNT	GNSS stations for which residuals of the Helmert transformation do not exceed 1 cm for the horizontal and 3 cm for the vertical coordinates	Set of the SLRF2014 core stations reduced by stations showing systematic effects McDonald (7080), Changchun (7237), Wettzell (8834) excluded
Pole coordinates	X pole, Y pole; two parameters per each component per day	
UT1-UTC	Initial value fixed to the a priori from IERS-14-C04, drift of the UT1-UTC freely estimated (denoted as LoD)	
Geocenter coordinates	X, Y, Z per each day	
Orbital elements	GNSS orbit parameters: 6 Keplerian, 5 ECOM: D_0, Y_0, B_0, B_{1C}, B_{1S} + stochastic orbit parameters in the radial, along-track, and cross-track directions every 12 h	
Troposphere	Site-specific zenith total delay (1 h), gradients (12 h)	-
Range Biases	-	Annual range biases calculated for each satellite-station pair; resubstituted and strongly constrained to a priori in the combined solution

- GNSS-specific parameters.

Software: Bernese GNSS Software, modified version

Processing strategy – estimated parameters

- **Common parameters** – one set estimated based on two types of observations.

Parameter	GNSS	SLR
Station coordinates	X, Y, Z for each GNSS and SLR station with NNR/NNT constraints for datum defining stations	
Datum defining stations for NNR/NNT	GNSS stations for which residuals of the Helmert transformation do not exceed 1 cm for the horizontal and 3 cm for the vertical coordinates	Set of the SLRF2014 core stations reduced by stations showing systematic effects McDonald (7080), Changchun (7237), Wettzell (8834) excluded
Pole coordinates	X pole, Y pole; two parameters per each component per day	
UT1-UTC	Initial value fixed to the a priori from IERS-14-C04, drift of the UT1-UTC freely estimated (denoted as LoD)	
Geocenter coordinates	X, Y, Z per each day	
Orbital elements	GNSS orbit parameters: 6 Keplerian, 5 ECOM: D_0, Y_0, B_0, B_{1C}, B_{1S} + stochastic orbit parameters in the radial, along-track, and cross-track directions every 12 h	
Troposphere	Site-specific zenith total delay (1 h), gradients (12 h)	-
Range Biases	-	Annual range biases calculated for each satellite-station pair; resubstituted and strongly constrained to a priori in the combined solution

- GNSS-specific parameters.
- SLR-specific parameters.

Software: Bernese GNSS Software, modified version

Processing strategy – estimated parameters

- **Common parameters** – one set estimated based on two types of observations.
- The combination is done at the normal equation level using the cumulative set of SLR and GNSS observations. All parameters are estimated with no pre-elimination, allowing for geocenter, ERP, and orbital space-ties.
- GNSS-specific parameters.
- SLR-specific parameters.

Parameter	GNSS	SLR
Station coordinates	X, Y, Z for each GNSS and SLR station with NNR/NNT constraints for datum defining stations	
Datum defining stations for NNR/NNT	GNSS stations for which residuals of the Helmert transformation do not exceed 1 cm for the horizontal and 3 cm for the vertical coordinates	Set of the SLRF2014 core stations reduced by stations showing systematic effects McDonald (7080), Changchun (7237), Wettzell (8834) excluded
Pole coordinates	X pole, Y pole; two parameters per each component per day	
UT1-UTC	Initial value fixed to the a priori from IERS-14-C04, drift of the UT1-UTC freely estimated (denoted as LoD)	
Geocenter coordinates	X, Y, Z per each day	
Orbital elements	GNSS orbit parameters: 6 Keplerian, 5 ECOM: D_0, Y_0, B_0, B_{1C}, B_{1S} + stochastic orbit parameters in the radial, along-track, and cross-track directions every 12 h	
Troposphere	Site-specific zenith total delay (1 h), gradients (12 h)	-
Range Biases	-	Annual range biases calculated for each satellite-station pair; resubstituted and strongly constrained to a priori in the combined solution

Software: Bernese GNSS Software, modified version

Processing strategy – weighting strategies

- Microwave GNSS solution **(M1).**
- The accuracy of microwave observations is assessed based on the a posteriori sigma of unit weight for the **microwave Galileo** carrier phase solutions, i.e., **1.5 mm**. The accuracy of laser ranging to GNSS is assessed based on the SLR residuals to GNSS satellites (https://govus.pl/slr). For the best-performing stations, the STD of the **SLR** residuals is at the level of **15 mm (W1)**.
- The intermediate case **(W2)**: increased contribution from SLR due to a lower number of tracking stations and observations.
- Equal weights for both types of observations **(W3).**

	σ_{GNSS} [mm]	$\frac{\sigma_{GNSS}}{\sigma_{SLR}}$
M1	1.5	-
W1	1.5	$\frac{1}{10}$
W2	1.5	$\frac{1}{4}$
W3	1.5	$\frac{1}{1}$

Reduction of the formal error of the semi-major axis – **solution precision**

- Introducing **SLR observations diminishes the formal errors** of the semi-major axis. SLR provides direct information about ranges to satellites.

- **The higher the SLR weights** the **greater the reduction** of the formal error of the semi-major axis.

- **The more SLR observations the higher the reduction of the semi-major axis formal errors**.

- The addition of **50 SLR** observations to the GNSS solution **diminishes the mean error** by **6, 15, and 29%** for the Galileo-FOC, and **10, 25, and 46%** for the Galileo-IOV in W1, W2, and W3, respectively.

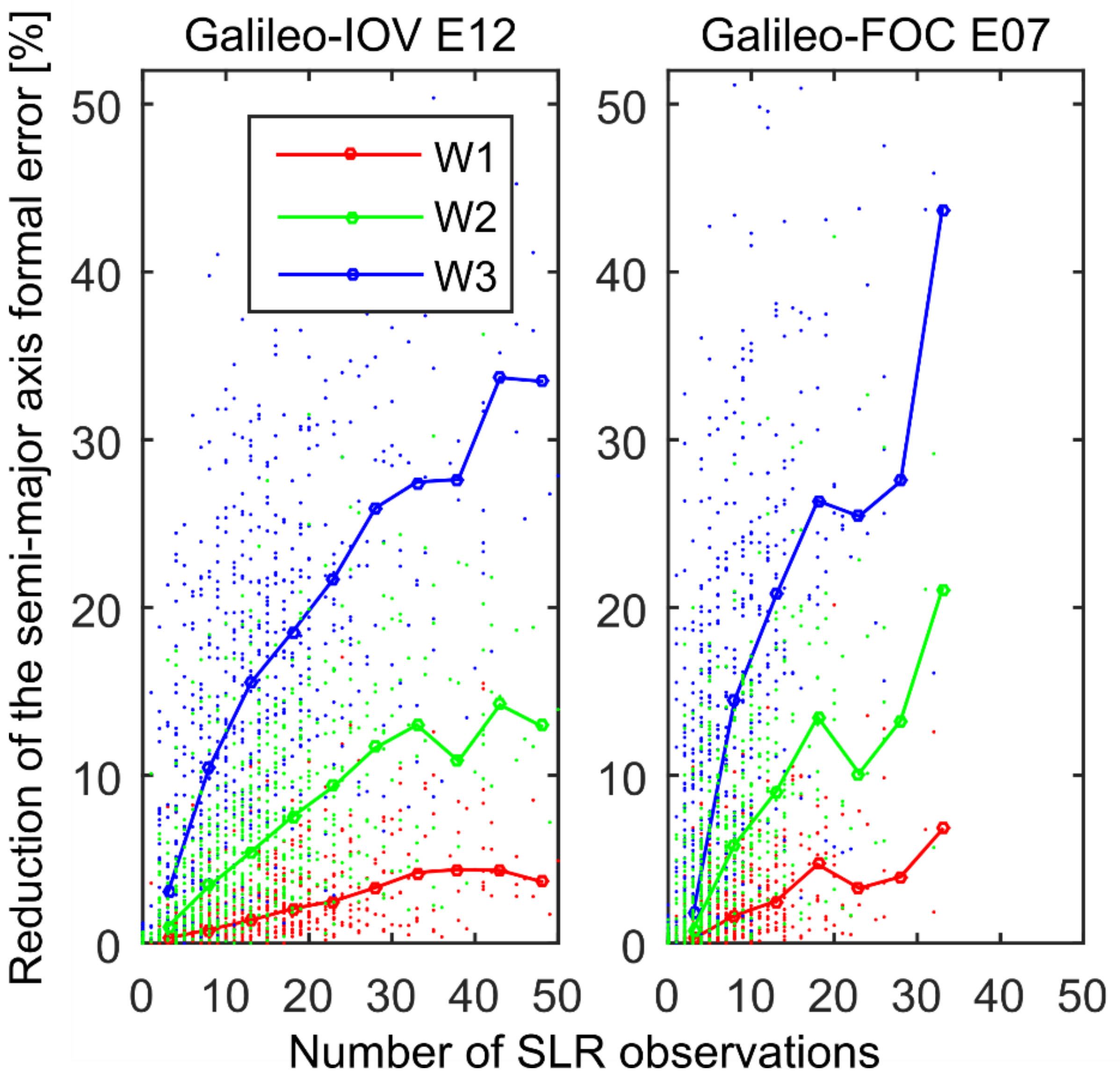

Reduction of the formal error of the semi-major axis – **solution precision**

- The semi-major axis formal error **depends on the β angle**.

- For the solutions W2 and W3, the β-angle dependency is distinct, especially for the eclipsing periods, |β| < 12°, and for |β| > 60°.

- When SLR added, the mean formal error of the semi-major axis is diminished by **5, 12, and 23% for W1, W2, and W3, respectively, for |β| = 78°**.

- Thus, the weakest parts of Galileo orbits (with lowest and highest |β|) are stabilized by SLR.

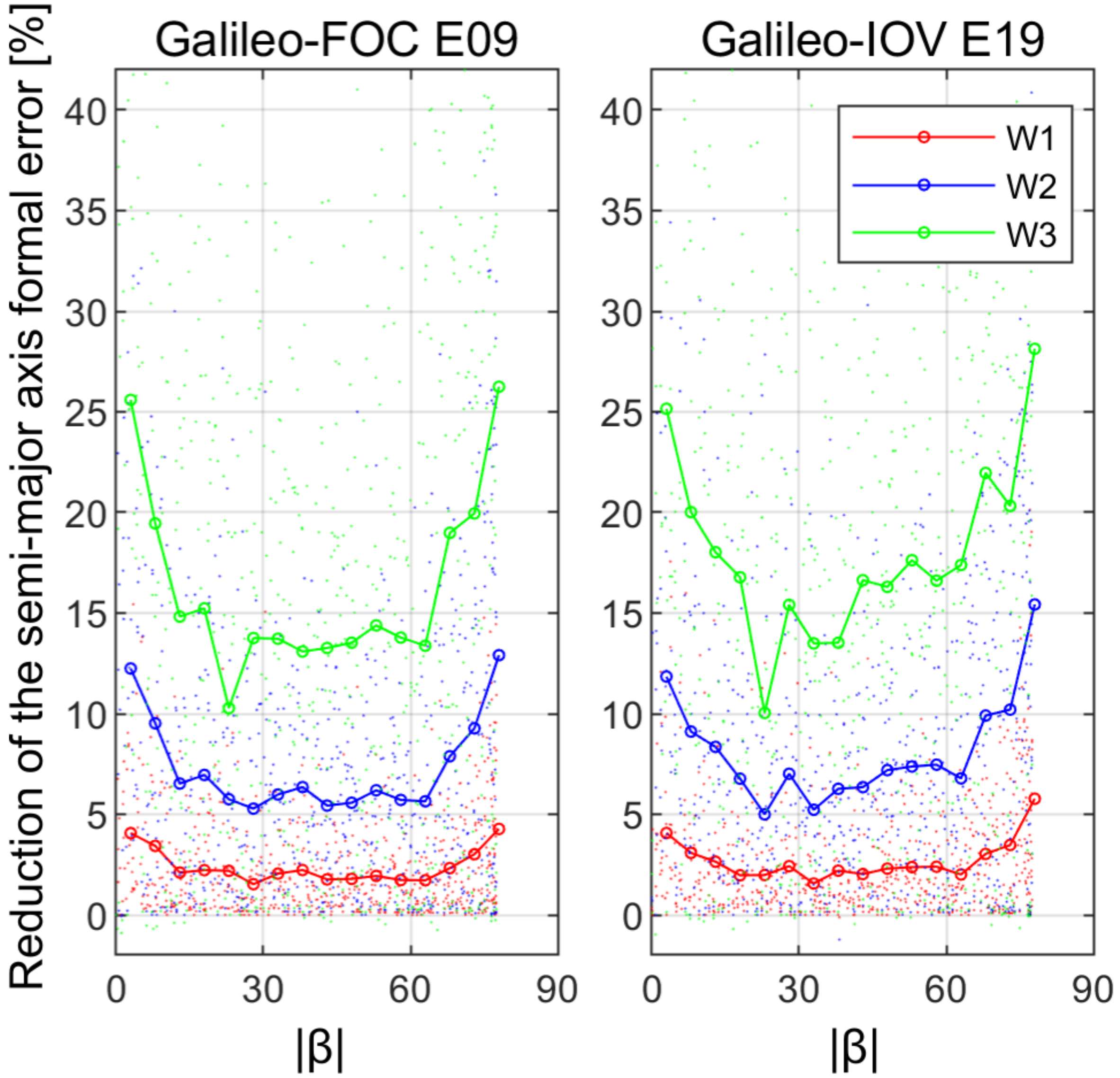

SLR residuals – **solution accuracy**

- **SLR residuals depend on the β angle**, especially, for the Galileo-IOV satellites.

- The microwave solution (**M1**) and combined solution with the lowest weights for SLR (**W1**) **are very similar.**

- **Solutions W2** and **W3 have SLR residuals closest to zero.**

- For W3, the offset of the SLR residuals reaches almost 0, however, this solution is **incorrectly dominated by SLR** because (next slide) …

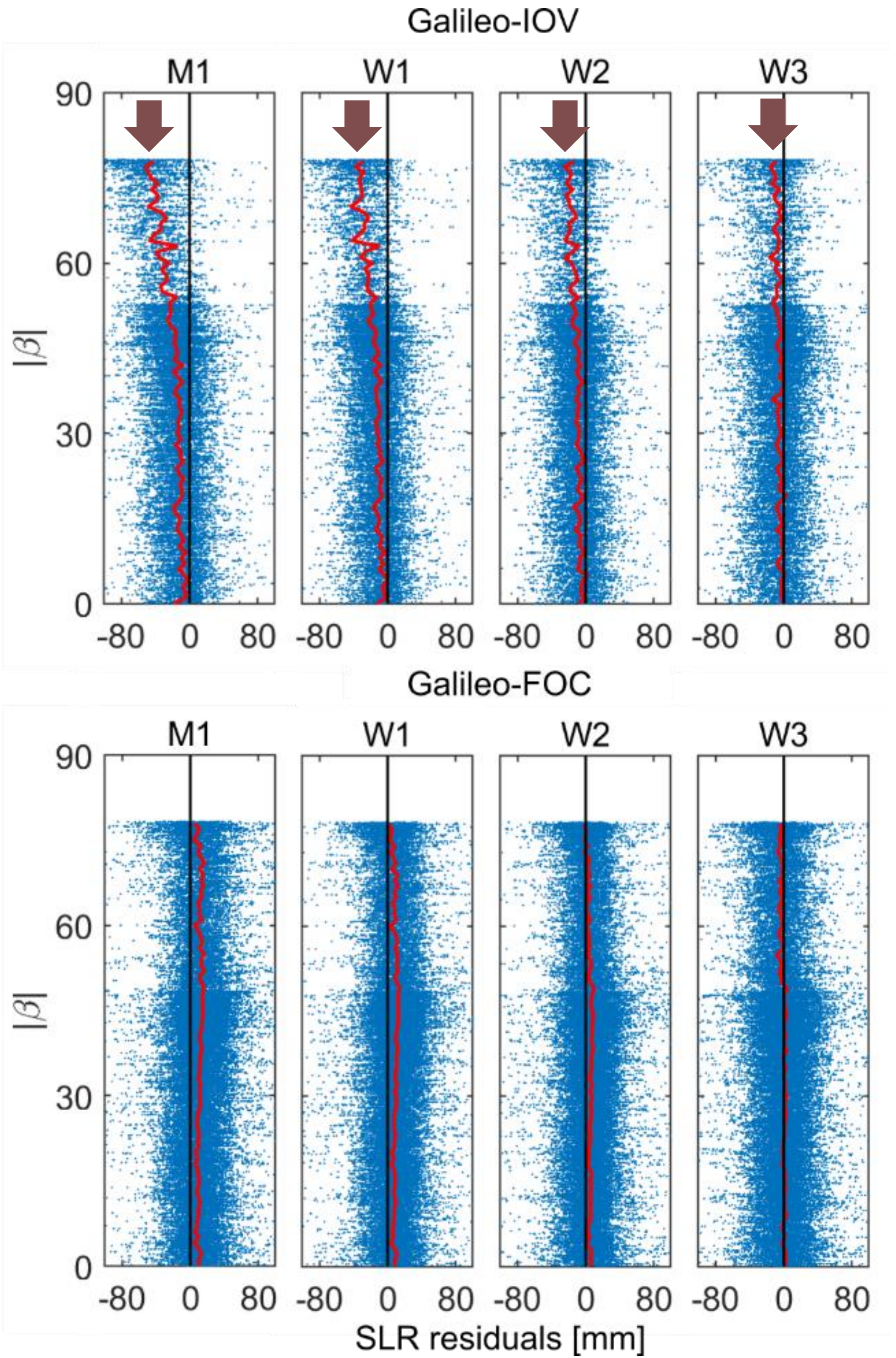

SLR residuals – **solution accuracy**

- …the number of **SLR residuals smaller than 2 cm** for the solution **W3 is lower** when compared to the solution **W2**. Thus, W2 is better than W3.

- Moreover, the **number of SLR residuals lower than 5 cm is higher for the solution W1 as compared to the solution W3** for the Galileo-FOC satellites.

- As a result, the best solution is **W2,** for which the number **SLR residuals lower than 2 cm** is **71.7%**.

For M1, W1, and W3 the numbers of SLR residuals below 2 cm are 60.6. 66.0, and 68.5%, respectively (FOC).

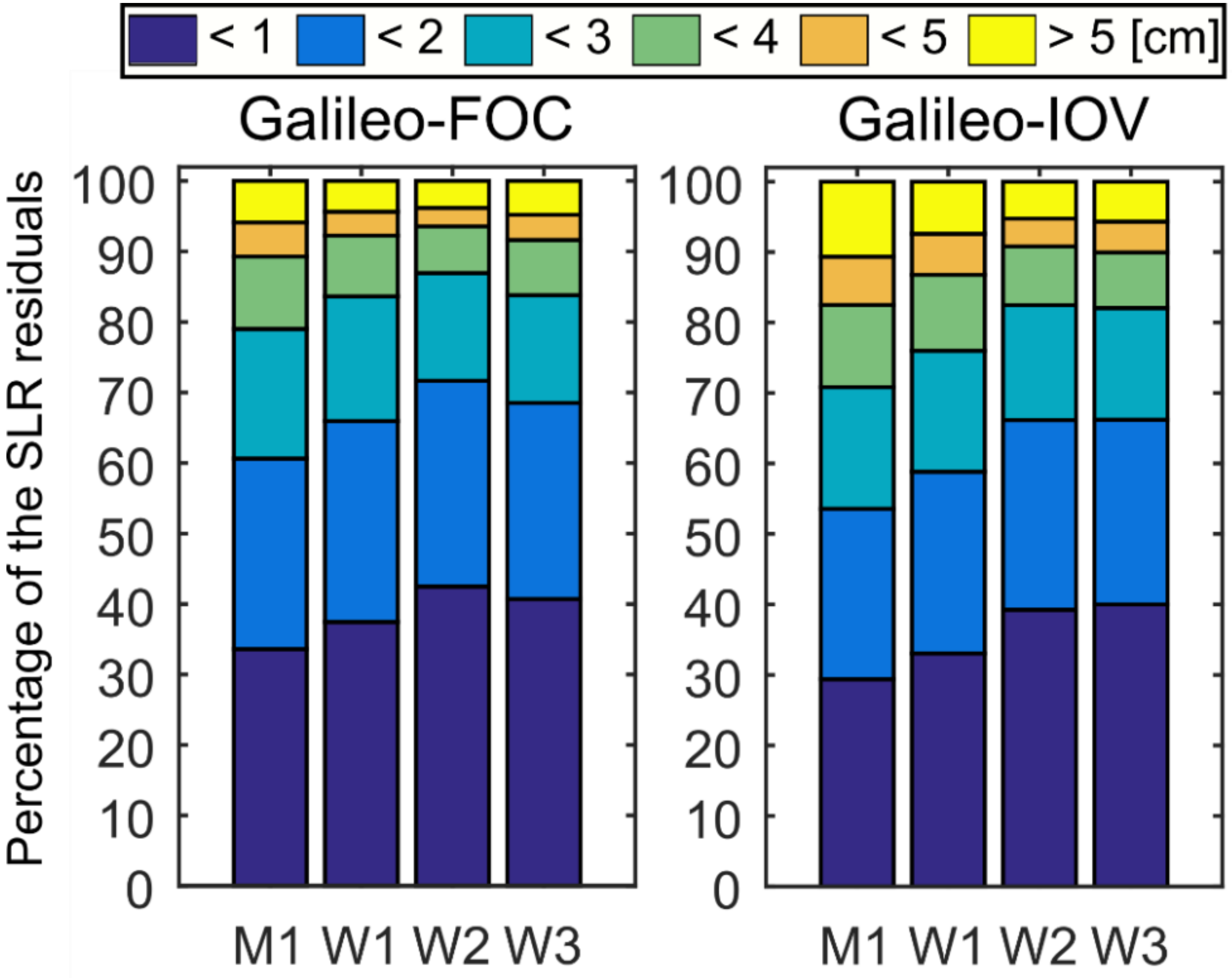

Number of SLR residuals smaller than 1, 2, 3, 4, 5 cm and above 5 cm in %.

SLR residuals – **solution accuracy**

- **W2** is characterized with the **lowest STD of SLR residuals** of all the solutions, especially for the Galileo-IOV when |β|>60°

[mm]	M1	W2
FOC (all sats)		
Mean	11.0	5.3
STD	26.6	24.4
IOV (all sats)		
Mean	-14.7	-8.5
STD	29.3	25.5
STD for β > 60°	36.3	29.6

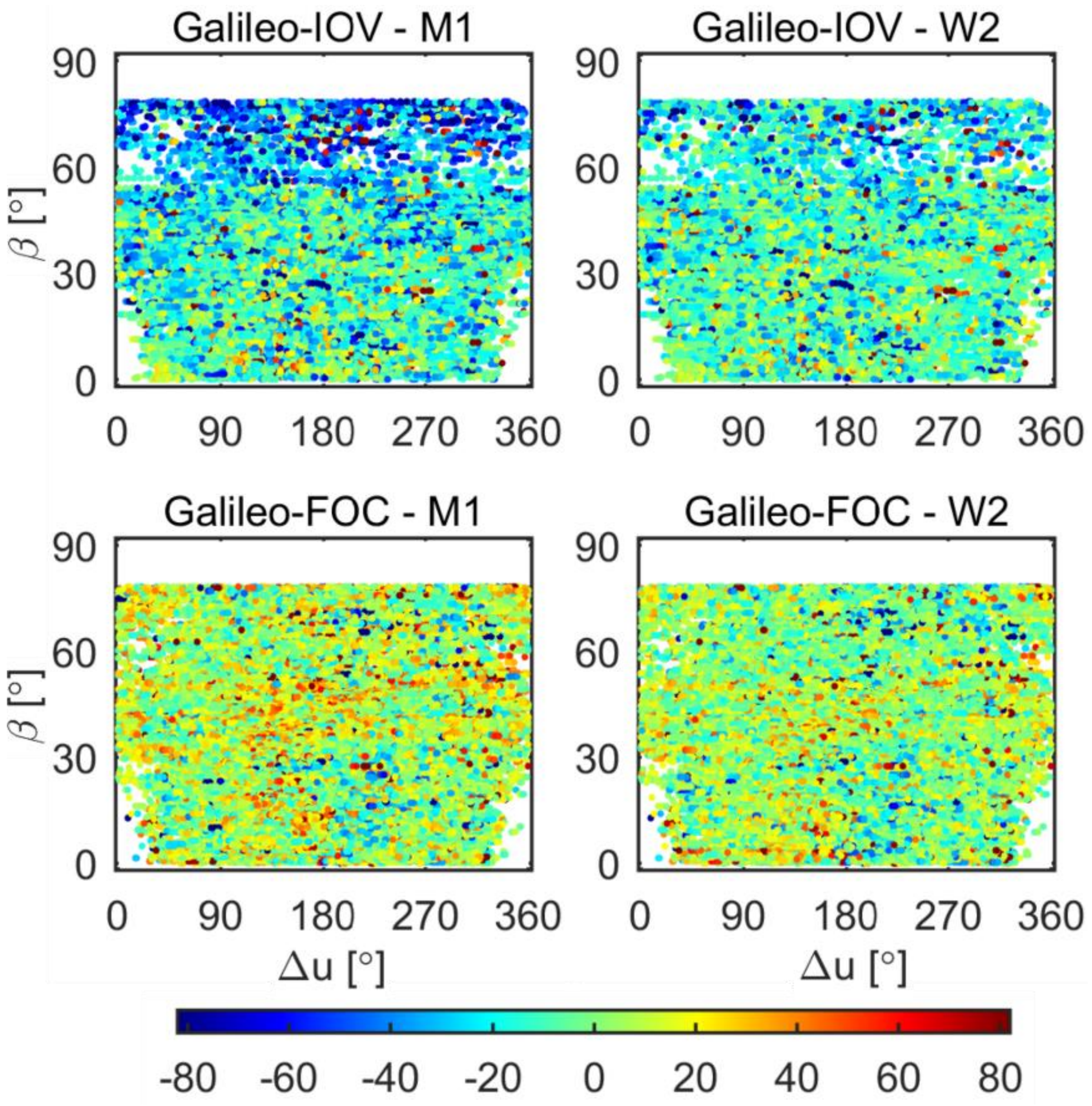

SLR residuals – **solution accuracy**

- **W2** is characterized with the **lowest STD of SLR residuals** of all the solutions, especially for the Galileo-IOV when |β|>60°

[mm]	M1	W2
FOC (all sats)		
Mean	11.0	5.3
STD	26.6	24.4
IOV (all sats)		
Mean	-14.7	-8.5
STD	29.3	25.5
STD for β > 60°	36.3	29.6

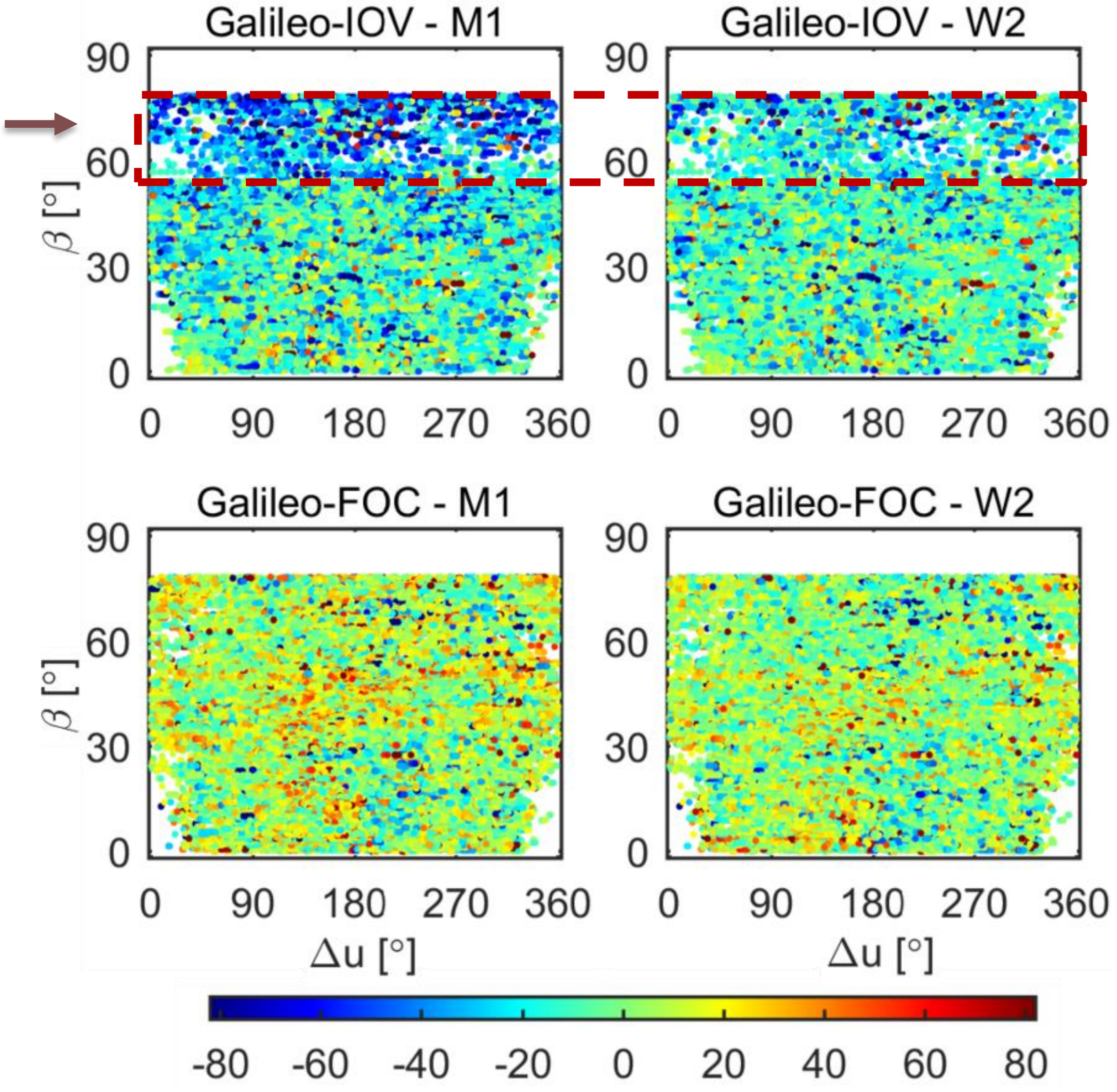

What happens during high β-angles? – Empirical orbit parameters

- **SLR technique stabilizes the orbit**, especially in the **radial** direction which is directly measured.

- Empirical parameters (such as estimated in the ECOM model) are supposed to absorb the unmodelled orbit perturbations.

- **For high β-angles, the direction B** of the ECOM model **approximates the radial** direction. B is perpendicular to D (Sun direction) and Y (solar panel axis).

- **Estimated values of the constant acceleration in B (B_0) are lower (closer to 0 value) for all the combined solutions** than for microwave M1.

$$\begin{bmatrix} D \\ Y \\ B \end{bmatrix} = \begin{bmatrix} D_0 \\ Y_0 \\ B_0 + B_{1C}\cos\Delta u + B_{1S}\sin\Delta u \end{bmatrix}$$

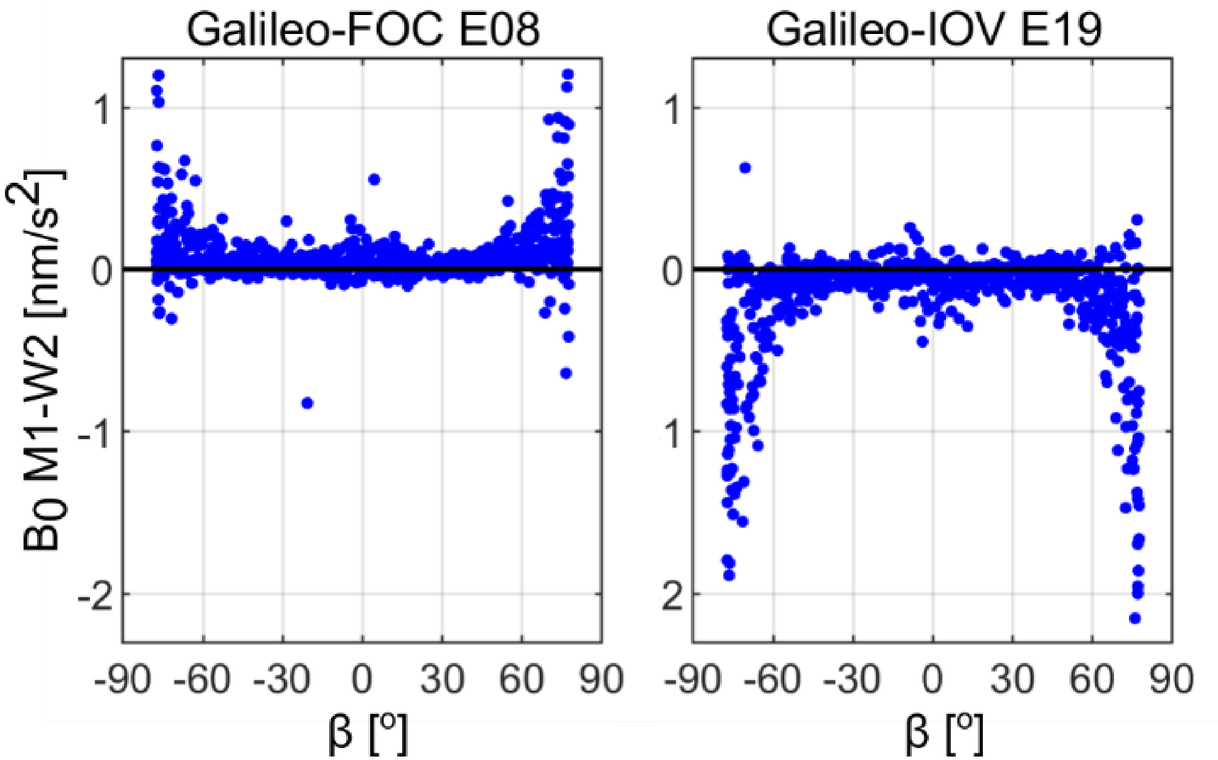

Differences between empirical parameter B_0 estimated in scenarios M1 and W2 for the Galileo-FOC E08 (left) and Galileo-IOV E19 (right) as a function of β angle

What happens during high β-angles? – Orbit positions

- The **differences between satellites positions** calculated using microwave (**M1**) and combined (**W2**) solutions **in the radial direction** are consistent with the B_0 differences. In the case of Galileo-FOC, **the differences reach up to 3.9 cm with the STD at the level of 1.3 cm for |β| > 60°.**

- In the along-track direction, large differences occur during the eclipsing periods. The cross-track component seem to be most insensitive for the addition of the SLR observations.

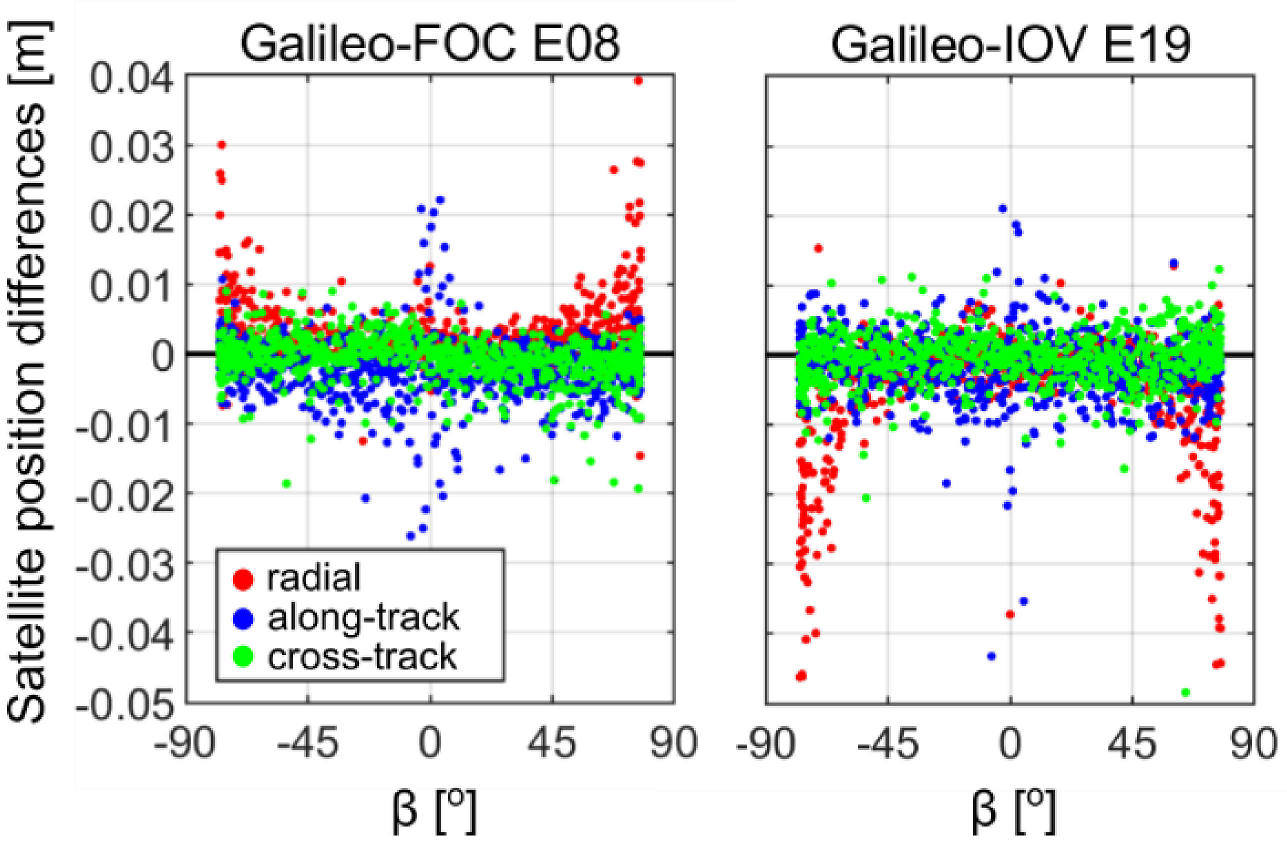

Differences between satellite positions determined using the microwave (M1) and combined (W2) solutions decomposed into the radial, along-track, and cross-track directions for Galileo-FOC E08 (left) and Galileo-IOV E19 (right)

Quality of the orbit prediction (2nd day of the predicted orbit)

- Scenario W1 provides the best orbit prediction results with 52.9, 54.4, and 55.1% of better prediction cases in the radial, along-track, and cross-track directions, respectively, when compared to M1.
- W3 is inferior as compared to the solution M1 with the improvement of the orbit prediction at the level of 51.5, 36.7, and 40.7% for the radial, along-track, and cross-track components.

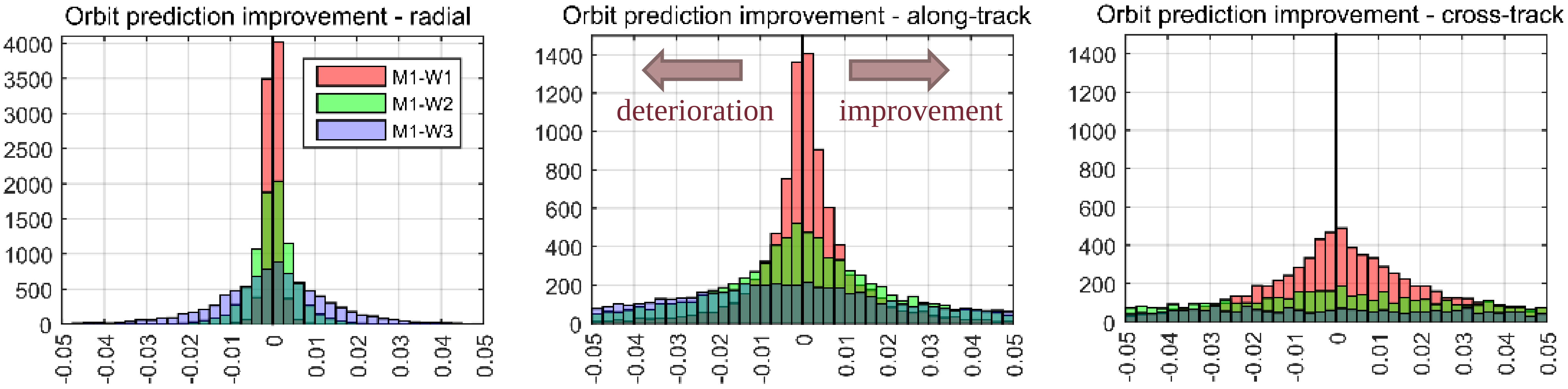

Orbit prediction improvement decomposed into the radial (top) along-track (middle) and cross-track (bottom). The improvement is calculated for all the combined scenarios with respect to the microwave (M1) solution and expressed in meters (horizontal axis). The vertical axis denotes the number of solutions

Quality of the orbit predictions

- In the predictions, the **most stable is the cross-track** component for which the median STD is at the level 4.8 and 5.9 cm for E02 and E19, respectively.

- The largest difference are for the along-track component for high β angles

- The median STD for the radial component is at the level of 6.5 and 8.9 cm for E02 and E19, respectively.

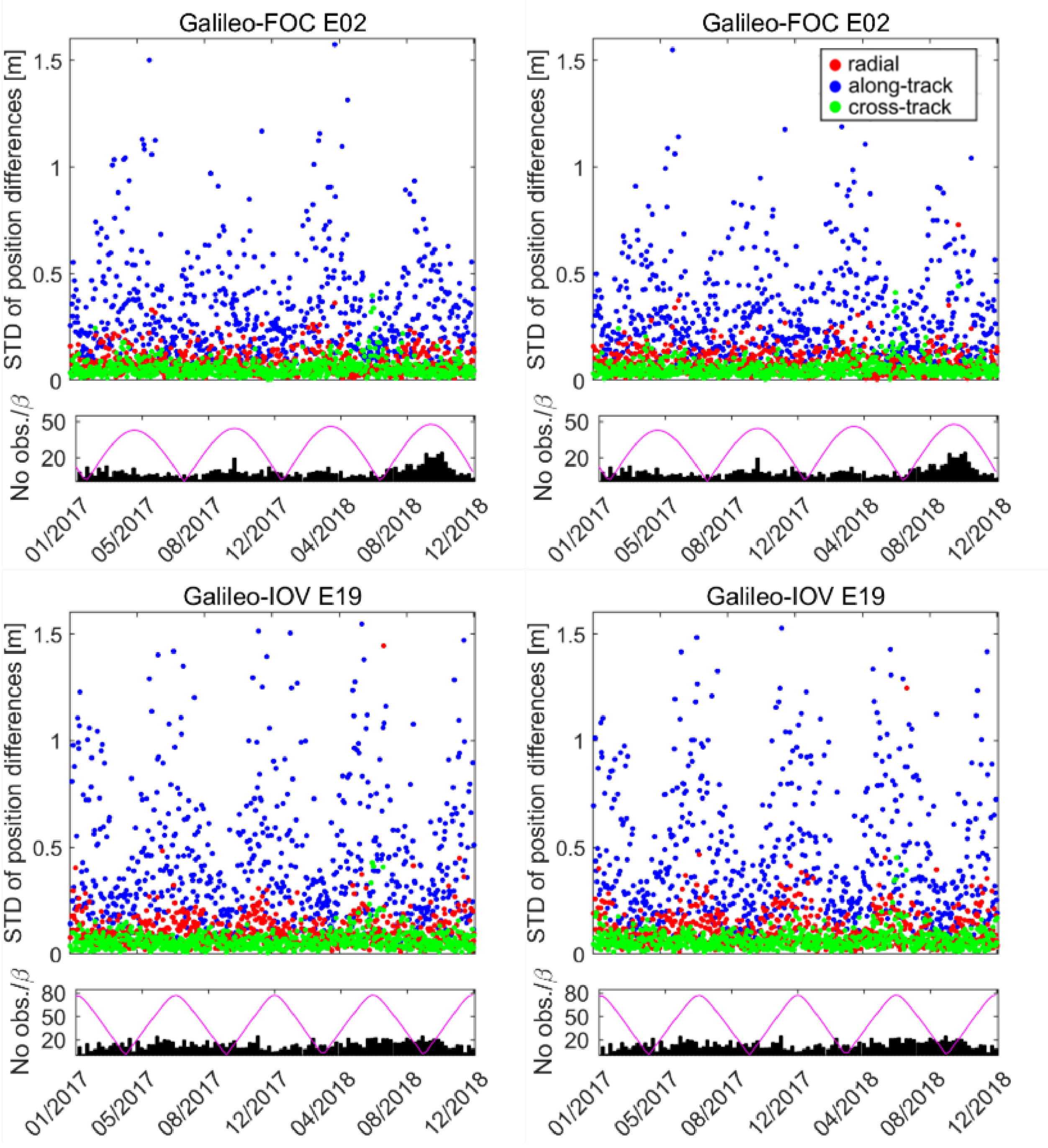

Top: STD of the differences between predicted and observed orbits from solution W2 (left) and M1 (right); Bottom: the number of SLR observations and the β angle

Summary

The influence of the SLR observations on the combined SLR+GNSS orbits is not spectacularly large due to the limited number of observations which are provided, in the best case, by thirteen SLR stations. An increased number of SLR observations to GNSS satellites would be hugely beneficial for the combined GNSS and SLR solution.

Introduction of the SLR observations to the combined GNSS and SLR solutions stabilizes the orbit in the radial direction. The largest improvement is for eclipsing periods and for $|\beta|>60°$, which are the weakest parts of GNSS-based orbits.

Combined GNSS and SLR-to-Galileo solution calculated using scenario W2 (sigma ratio GNSS:SLR as 1:4) provides the Galileo orbits with RMS of SLR residuals at the level of 25 mm. Space tie SLR+GNSS onboard Galileo is possible, however, requires the utmost consistent orbit, parameter, and data modeling.

Progress in the Galileo orbit accuracy based on the Galileo-IOV

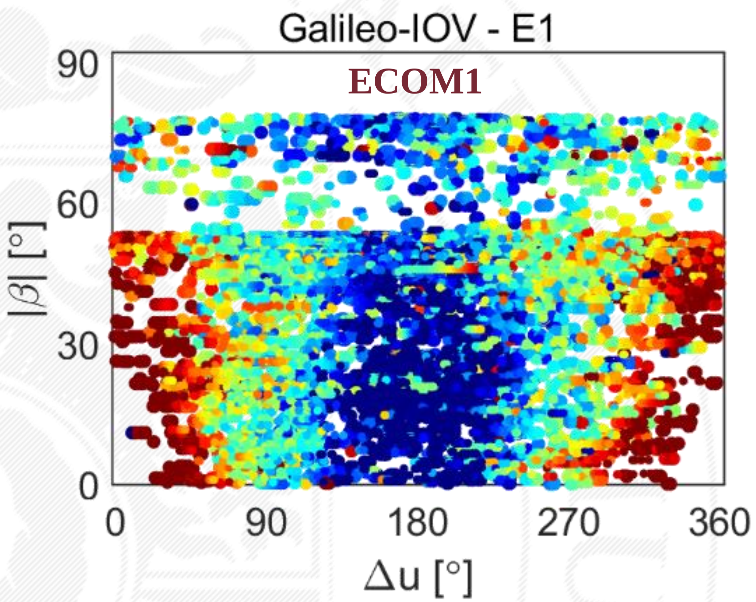

Progress in the Galileo orbit accuracy based on the Galileo-IOV

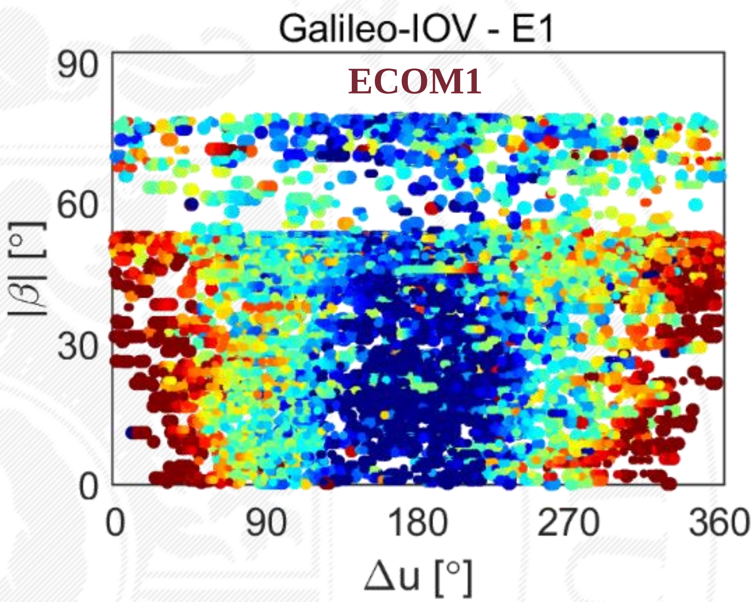

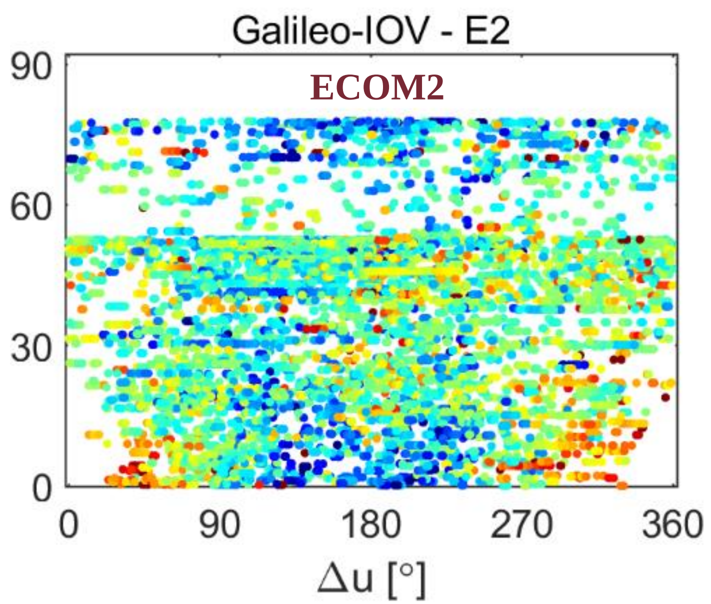

Progress in the Galileo orbit accuracy based on the Galileo-IOV

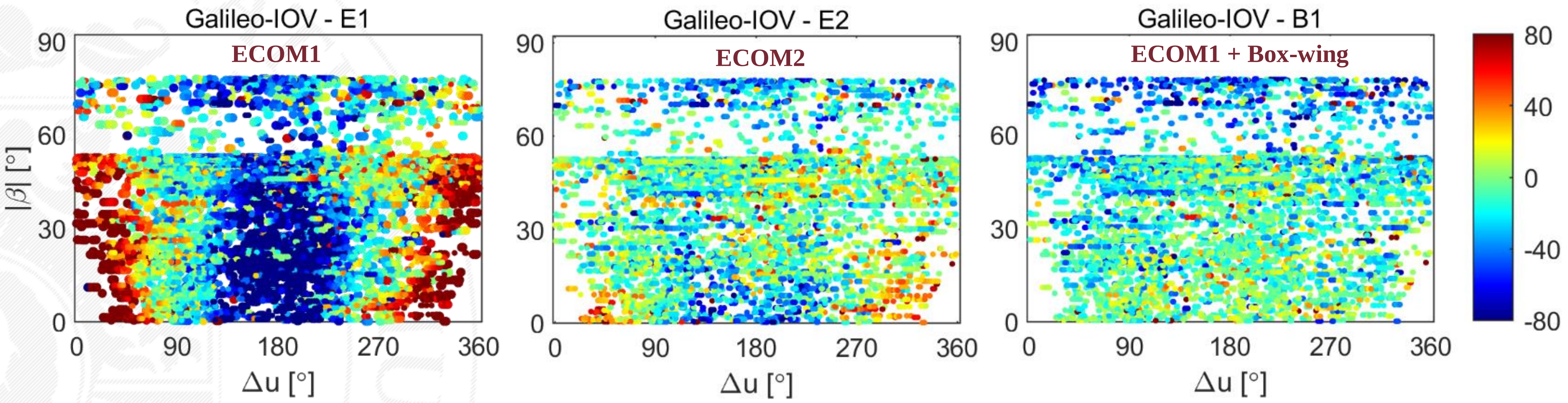

Progress in the Galileo orbit accuracy based on the Galileo-IOV

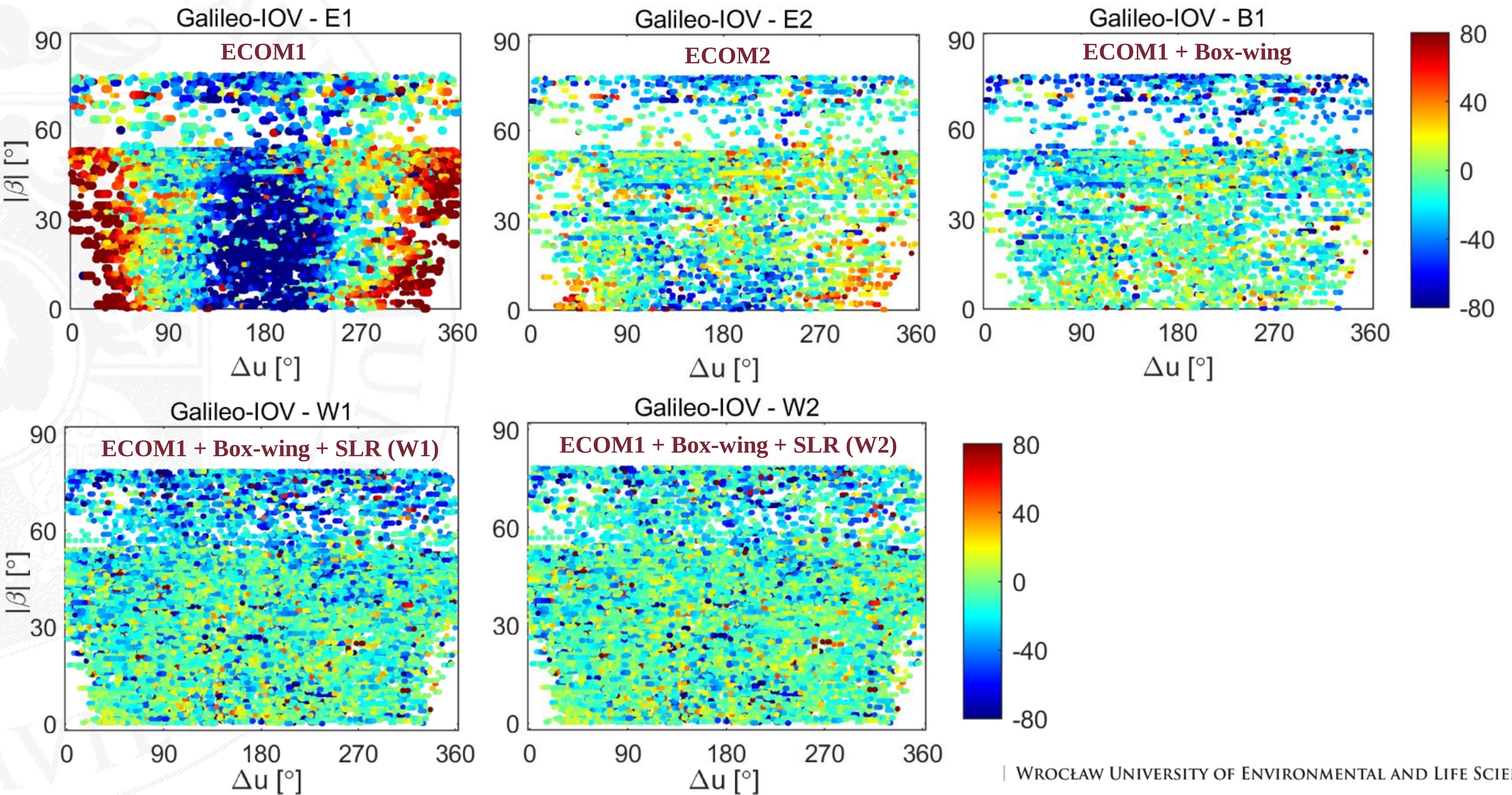

Progress in the Galileo orbit accuracy based on the Galileo-IOV

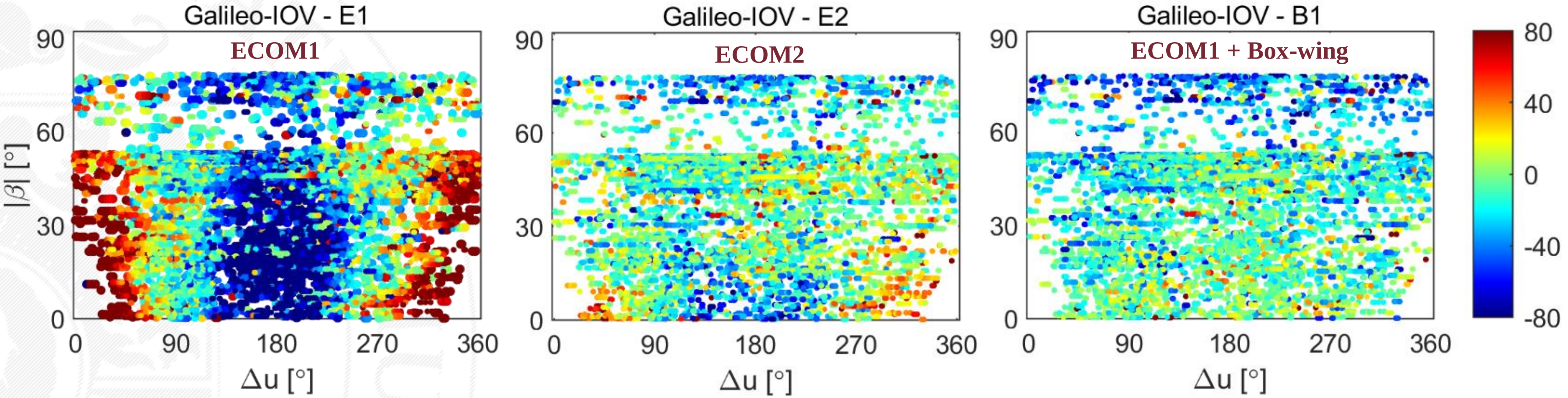

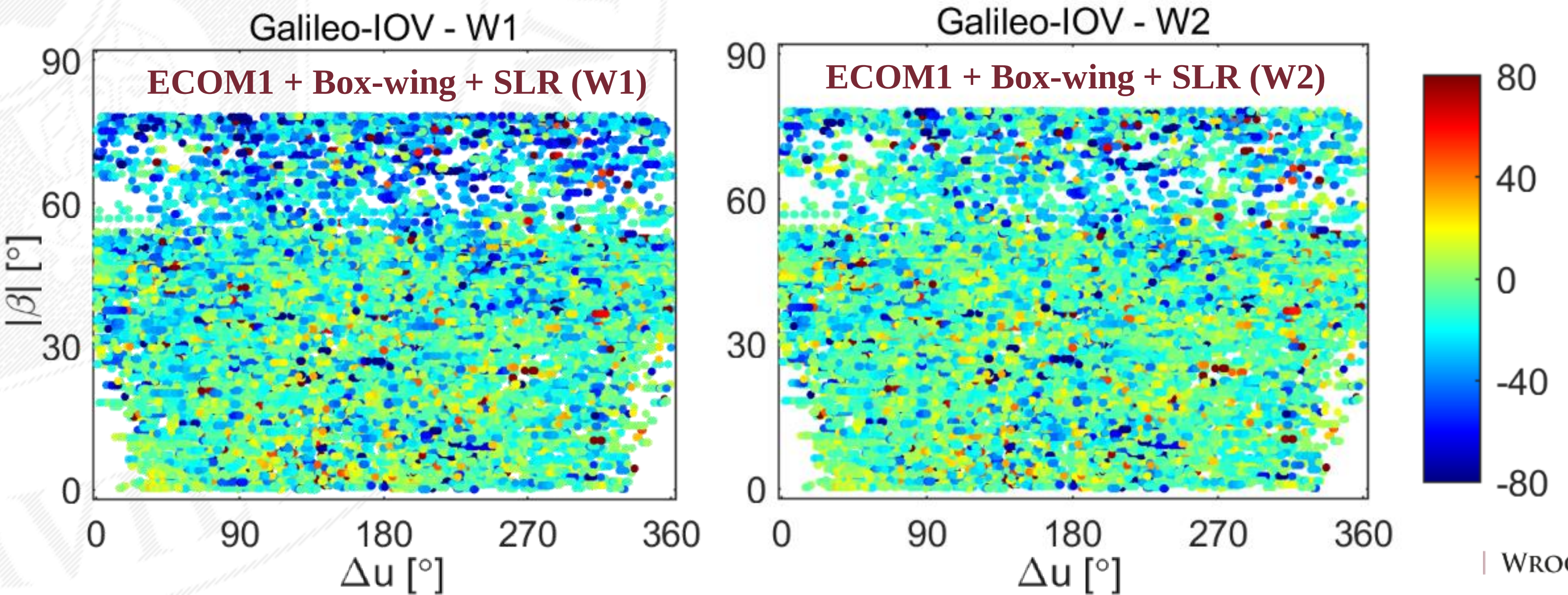

[mm]	E1	W2
Mean	-7.0	-8.5
STD	62.7	25.5
STD $\|\beta\| < 12^o$	72.3	27.4
STD $\|\beta\| > 60^o$	38.8	29.6

Thank you for your attention

Grzegorz Bury
grzegorz.bury@upwr.edu.pl